Karlsruher Institut für Technologie

Finite Element study on a Vickers cone crack

Open Access am KIT

by Gabriele Rizzi, Theo Fett

KIT SCIENTIFIC WORKING PAPERS 4

KIT – Universität des Landes Baden-Württemberg und nationales Forschungszentrum in der Helmholtz-Gemeinschaft

Institut für Angewandte Materialien, Karlsruher Institut für Technologie (KIT)

Impressum

Karlsruher Institut für Technologie (KIT)
www.kit.edu

2013

ISSN: 2194-1629

Abstract

During a Vickers indentation test in a glass surface, in most glasses a cruciform semi-elliptical crack system is generated. In the special case of silica conical cracks with small cone opening angles develop as a consequence of its anomalous densification behavior beneath the indentation contact. Since cone cracks are used in the determination of subcritical crack growth curves, it was of interest to compute the stress intensity factor K by using finite elements. In addition, also results on T-stress and crack opening behavior are reported.

Zusammenfassung

Vickerseindrücke in Glasoberflächen führen in der Regel zu gekreuzten halbelliptischen Oberflächenrissen. Wegen seines anomalen Verdichtungsverhaltens führen Vickerseindrücke in Quarzglas zu kegelförmigen Oberflächenrissen mit relativ geringen Öffnungswinkeln. Da derartige Risse bei der Bestimmung des unterkritischen Rißwachstums verwendet werden, war es von Interesse, die bruchmechanischen Belastungsparameter (Spannungsintensitätsfaktor, T-Spannung und COD-Verhalten) aus FE-Rechnungen zu bestimmen.

Contents

1. Introduction

Cone cracks are often applied for the investigation of crack growth in brittle materials. This topic was extensively studied in literature in numerous experimental investigations, mainly by Lawn and co-workers (see e.g. [1,2]). This holds for stable crack extension [3,4,5], quasi-static subcritical crack growth [6,7,8], and cyclic fatigue loading [9,10,11,12].

Whereas most tests were performed under sphere contacts, Sglavo and Green [8] studied crack growth on cone cracks in silica obtained by Vickers indentation, which clearly indicated a fatigue limit at a stress intensity factor of about $K \approx 0.3$ MPa$\sqrt{m}$.

Measurements by Wiederhorn and Bolz [13], Michalske *et al.* [14] and Muraoka and Abe [15] (the latter down to $K \approx 0.32$ MPa$\sqrt{m}$ and crack velocities of about 10^{-13}m/s) did not show such a behaviour for silica. In this context, it should be noted that the stress intensity factors for the cone cracks were determined experimentally in contrast to the other specimens, for which solutions were available from handbooks or FE analyses.

It was the reason of our study to compute the loading parameters of a cone crack by a FE analysis for the special cone geometry of Fig. 1 as was reported in [8]. From this image we can conclude a cone-opening angle of 80°, a crack length of 67µm and a cone radius at the surface, *b*, in the order of about 5-7µm.

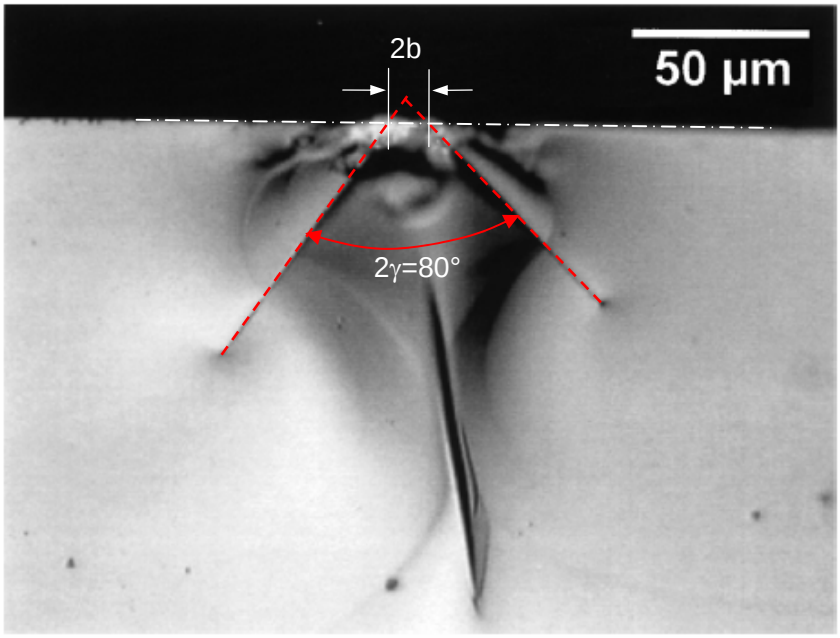

Fig. 1 Cone crack in silica from Sglavo and Green [8], subcritically grown under an indentation load of 9.81N for 120s.

2. Finite Element study

2.1 Stress intensity factors

The geometry of our FE-model is given in Fig. 2. The case of a semi-infinite body with a cone crack was realized by a FE mesh of about 1300 elements with 3900 nodes. The specimen was chosen to be a cylinder of radius 100*b* and thickness 200*b*. Solid continuum elements (8-node biquadratic) were chosen and the computations carried out with ABAQUS Version 6.8.

The pressure distribution under the indenter was prescribed as

$$p(x) = p_0 \sqrt{1-(x/r)^2} \tag{1}$$

resulting in the total indentation load of

$$P = \frac{2\pi}{3} p_0 r^2 \tag{2}$$

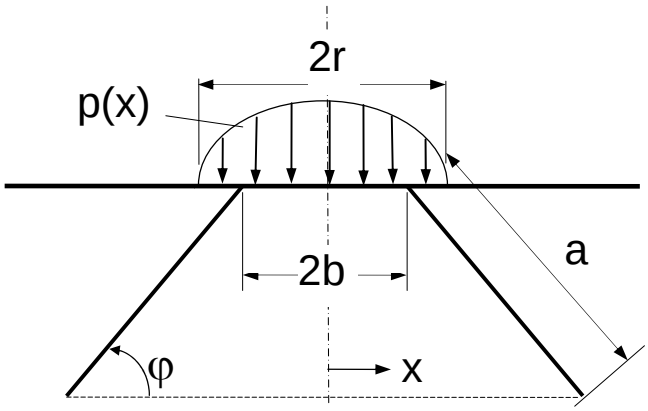

Fig. 2 Cone crack modeled by FE; a) contact area replaced by an equivalent circle, maximum pressure p_0 at x=0 (φ=50°), plate thickness: 400*b*.

Finite Element results are shown in Fig. 3 for different values of *a*/*b* and *r*/*b*. Figure 3a gives the normalized mode-I stress intensity factors K_I as a function of *r*/*b*. The related mode-II contributions K_{II} are the plotted in Fig. 3b. These results were obtained under the condition of freely sliding crack surfaces without any friction and roughness interaction. Mode-II stress intensity factors disappear in the region of 1.6<*r*/*b*<1.9. According to the theory of Cotterell and Rice [16], the straight crack in Fig. 1 must fulfill the condition K_{II}=0 at least in the phase of stable crack extension.

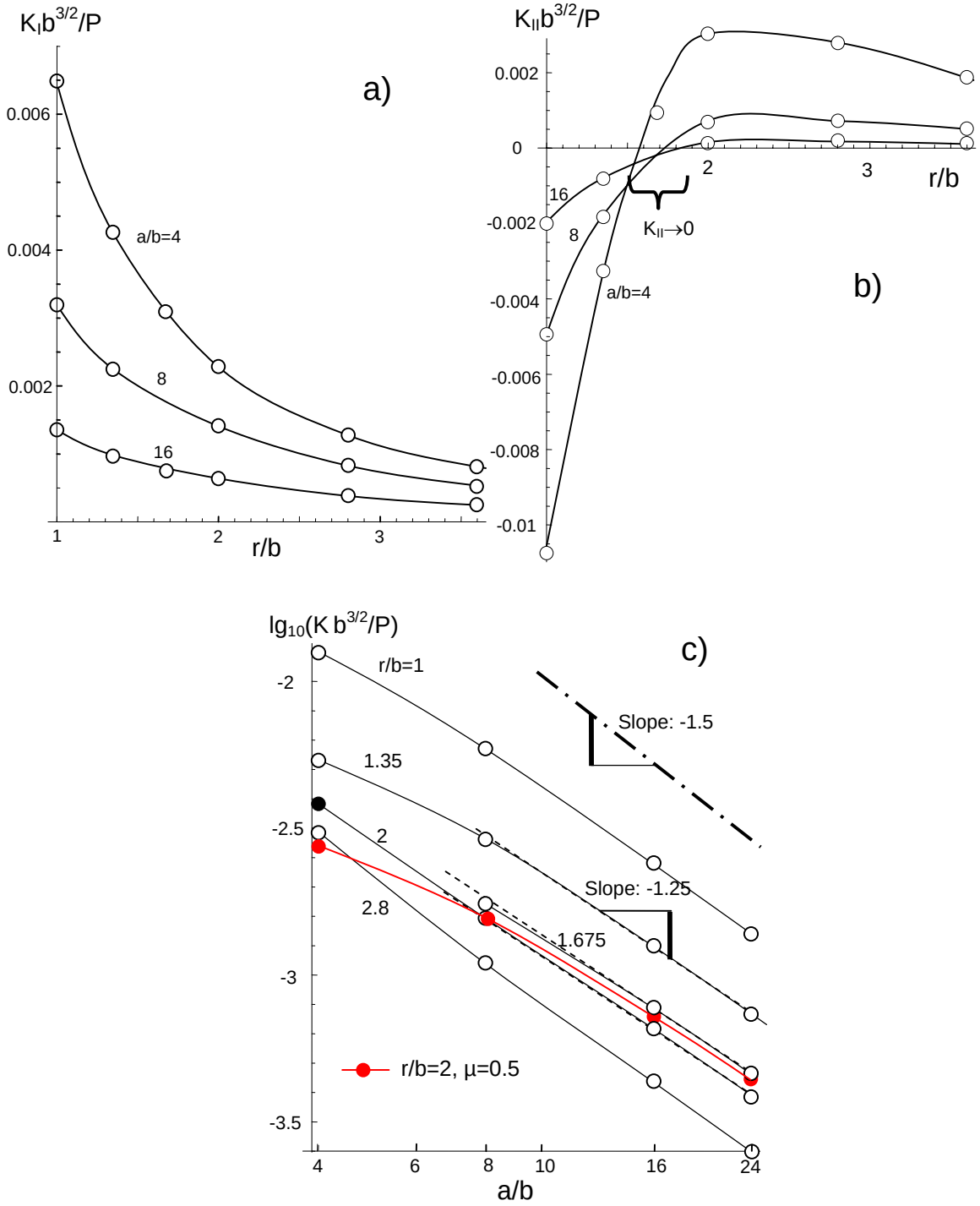

Fig. 3 Some of the Finite Element results for the cone crack, a) mode-I stress intensity factor, b) mode-II stress intensity factor contribution, c) logarithmic plot of the effective stress intensity factor K representing the energy release rate G via eqs.(3) and (4). The single solid circle shows the effect of a finite friction coefficient of μ=0.5 between the crack surfaces for a/b=16 and r/b=2. The dashed lines represent the approximation by eq.(5).

The energy release rate, G, defined as

$$G = \frac{K_I^2 + K_{II}^2}{E} \tag{3}$$

is shown in Fig. 3c where G is represented by an effective stress intensity factor K via

$$K = \sqrt{K_I^2 + K_{II}^2} \tag{4}$$

In the range of $1.35<r/b<2$ and $a/b>8$ the FE-results can be simply described by

$$\frac{Kb^{3/2}}{P} \cong f\left(\frac{r}{b}\right) \times \left(\frac{a}{b}\right)^{-5/4} \tag{5}$$

as illustrated by the dashed lines.

The effect of finite crack-surface friction is shown in Fig. 3c for a crack of a/b=16, r/b=2 for a friction coefficient of μ=0.5 (red symbols and curve). Since the effect of less than 10% in G is small, although for the friction coefficient a high value was chosen, the friction effect was neglected for the evaluation.

2.2 T-stress represented by the biaxiality ratio

In addition to the singular stress field represented by K also a strong constant stress term (so-alled T-stress term) is present. This stress has the only stress component $\sigma_{xx}=T$. The total near-tip stress field is then given as

$$\sigma_{ii} = \frac{K_{tip}}{\sqrt{2\pi r}} g_{ii}(\varphi) + T \tag{6}$$

where r is the crack-tip distance and g_{ii} are the well known geometric functions depending on the polar angle φ.

The T-stress results are shown in Fig. 4 in the load-independent representation by the biaxiality ratio β as proposed Leevers and Radon [17]

$$\beta = \frac{T\sqrt{\pi a}}{K_I} \tag{7}$$

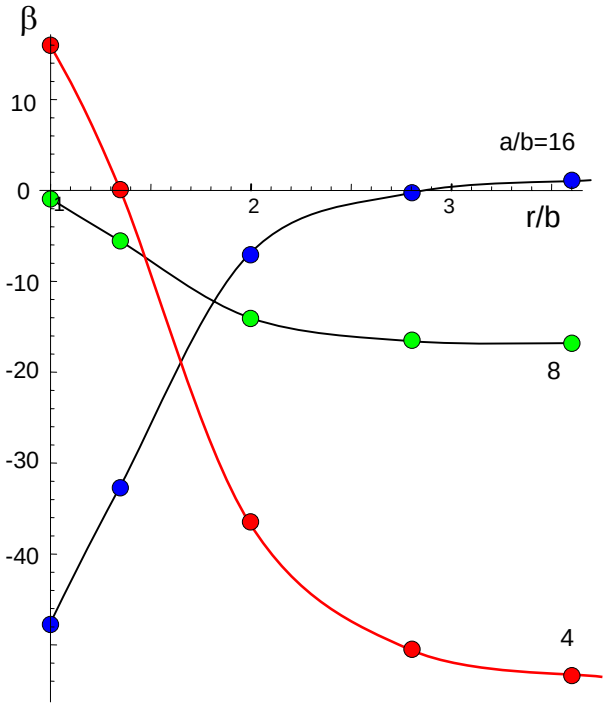

Fig. 4 T-stress term expressed by the biaxiality ratio β according to eq.(7).

2.3 Crack opening displacements

From earlier FE-studies on cone cracks at wider cone opening angles of φ=90°-γ=15-35° [10, 12, 18] (for γ see Fig. 1), the authors are aware that in the surface region of a cone crack the crack was closed although near the tip a positive displacement occurred resulting in a positive K_I-value.

The crack opening displacements for the crack with a/b=4 are plotted in Fig. 5. The upper sequence of crack profiles illustrates the case in which crack surface interpenetration is allowed. The profiles for r/b=1 and 1.35 show positive displacements in the crack-tip region, i.e. positive stress intensity factors, whereas for r/b=2 the displacement is negative. Near the specimen surface, the crack faces interpenetrate for r/b=1.35 and 2.

The realistic profiles obtained under rigid surface conditions are given by the lower sequence. Now, all cracks are open near the tip. In the cases where crack interpenetration occurred in the upper sequence, the crack is now closed.

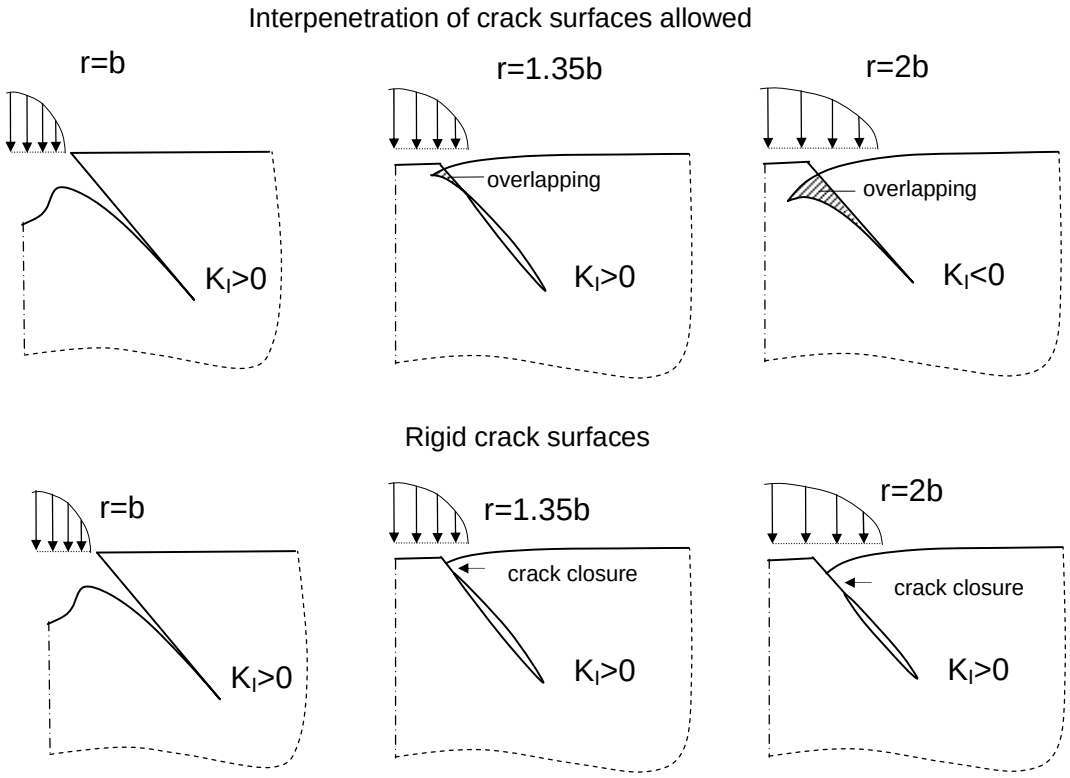

Fig. 5 Displacements for penetrating and rigid crack surfaces (crack length: a=4b).

3. Correction of K-values

The stress intensity factors for cone cracks were empirically determined in [8] by measuring the crack lengths of cracks introduced under different loads in silicon oil as the inert environment. In these tests the stress intensity factor must equal the fracture toughness of K_{Ic}=0.75 MPa√m. The measurements represented by

$$\hat{K} = \chi \frac{P}{a^{3/2}} \tag{8}$$

resulted in the coefficient χ=0.046. The stress intensity factor in eq.(8) is denoted $\hat{K}$ in order to distinguish theoretical and experimental results.

The FE-analysis establishes a stress intensity factor solution for different crack lengths obtained for one and the same indentation load P and a contact radius r kept constant during the subcritical crack growth test, i.e. for P=const and r/b=const. (Fig. 6a). In contrast, eq.(8) represents a K-solution for cracks with the increasing lengths obtained by increasing indentation loads, unavoidably accompanied by increasing contact radii (Fig. 6b). The different loading conditions must yield different K-values.

From the results in Fig. 3c and eq.(8) the stress intensity factor on the basis of the FE-computations, K, can be computed as a function of the empirically determined stress intensity factors $\hat{K}$.

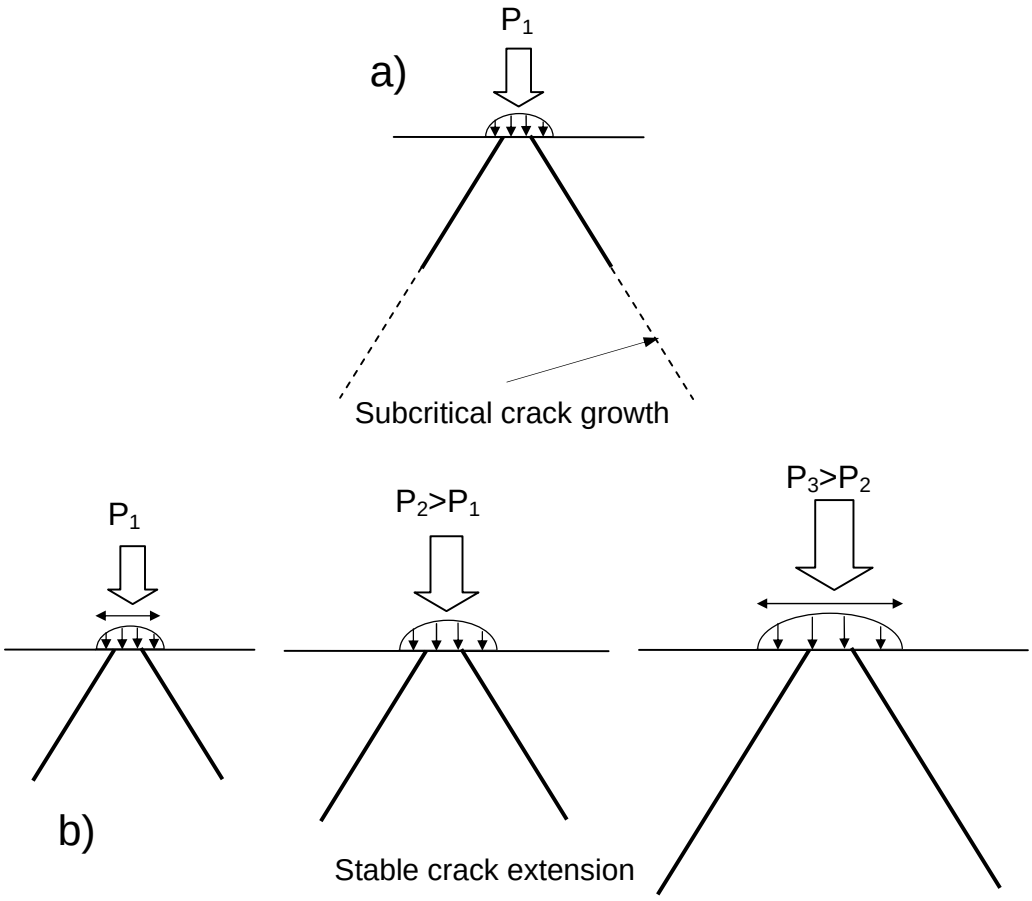

Fig. 6 a) Cone crack development under subcritical crack growth conditions at a constant load, b) calibration tests with stable crack extension at K=K_{Ic} under increasing indentation load P.

If the initial crack length is a_0, the condition K=K_{Ic} then reads in terms of eq.(5)

$$K = K_{Ic}\left(\frac{a_0}{a}\right)^{5/4} \tag{9}$$

From eq.(8) we obtain from the same condition

$$\hat{K} = K_{Ic}\left(\frac{a_0}{a}\right)^{3/2} \tag{10}$$

and by combining (9) and (10)

$$\frac{K}{\hat{K}} = \left(\frac{a}{a_0} \right)^{1/4} \tag{11a}$$

or by using (10) again

$$\frac{K}{\hat{K}} = \left(\frac{K_{Ic}}{\hat{K}} \right)^{1/6} \tag{11b}$$

References

1 Lawn, B., Wilshaw, T.R., Hartley, N.E.W., A computer simulation study of Hertzian cone crack growth, Int. J. Fract. **10**(1974), 1-16.

2 Lawn, B. and Wilshaw, T.R. Fracture of Brittle Solids, Cambridge University Press (1975).

3 Cai, H., Kalceff, M. A. S., Hooks, B. M., Lawn, B. R. and Chyung, K. (1994) Cyclic fatigue of a mica-containing glass- ceramic at Hertzian contacts. J. Mater. Res. **9**, 2654–2661.

4 Padture, N. P. and Lawn, B. R. (1995) Contact fatigue of a silicon carbide with a heterogeneous grain structure. J. Am.Ceram. Soc. **78**, 1431–1438.

5 T. Fett, E. Ernst, D. Munz, Contact strength measurements of bars under opposite sphere loading, J. Materials Science Letters **21**(2002), 1955-1957.

6 Kocer, C., Collins, R.E., The angle of Hertzian cone cracks, J. Amer. Ceram. Soc. **81**(1998), 1736-42.

7 Kocer, C., Collins, R.E., Measurement of very slow crack growth in glass, J. Amer. Ceram. Soc. **84**(2001), 2585-93.

8 V.M. Sglavo and D.J. Green, “Fatigue limit in fused silica,” J. Eur. Ceram. Soc. **21** (2001) 561-567.

9 Kim, D. K., Jung, Y. G., Peterson, I. M. and Lawn, B. R. (1999), Cyclic fatigue of intrinsically brittle ceramics in contact with spheres. Acta Mater. **42**, 4711–4725.

10 T. Fett, E. Ernst, G. Rizzi, D. Munz, D. Badenheim, R. Oberacker, Sphere contact fatigue of a coarse-grained Al2O3 ceramic, Fatigue Fract Engng Mater Struct **29**(2006), 1–11.

11 T. Fett, D. Creek, D. Badenheim, R. Oberacker, Crack growth data from dynamic tests under contact loading, J. Europ. Ceram. Soc. **24**(2004), 2049-2054.

12 T. Fett, E. Ernst, G. Rizzi, R. Oberacker, Failure of an Al2O3 ceramic under cyclic sphere contact loading, J. Mater. Sci. **39**(2004), 6817-6819.

13 S.M. Wiederhorn and L.H. Bolz, Stress Corrosion and Static Fatigue of Glass, J. Am. Ceram. Soc. **53**(1970) 543-548.

14 Michalske, T.A., Smith, W.L., Bunker, B.C., Fatigue mechanisms in high-strength silica-glass fibers, J. Am. Ceram. Soc., **74**(1991), 1993-96.

15 M. Muraoka and H. Abé, “Subcritical Crack Growth in silica Optical Fibers in a Wide Range of Crack Velocities,” J. Am. Ceram. Soc. **79**(1996), 51-57.

16 Cotterell, B., Rice, J.R., Slightly curved or kinked cracks, Int. J. Fract. **16**(1980), 155-169.

17 Leevers, P.S., Radon, J.C., Inherent stress biaxiality in various fracture specimen geometries, Int. J. Fract. **19**(1982), 311-325.

18 T. Fett, G. Rizzi, E. Diegele, Weight functions for cone cracks, Engng. Fract. Mech. **71**(2004), 2551-2560.

KIT Scientific Working Papers
ISSN 2194-1629

www.kit.edu